Journal of Photochemistry & Photobiology A: Chemistry 377 (2019) 130–137

Contents lists available at ScienceDirect

Journal of Photochemistry & Photobiology A: Chemistry

journal homepage: www.elsevier.com/locate/jphotochem

TiO_2 photocatalytic degradation of the flame retardant tris (2-chloroethyl) phosphate (TCEP) in aqueous solution: A detailed kinetic and mechanistic study

A.M. Abdullah, Kevin E. O'Shea*

Department of Chemistry and Biochemistry, Florida International University, Miami, FL 33199, United States

ARTICLE INFO

Keywords:
Organophosphate ester
Flame retardant
Tris (2-chloroethyl) phosphate
Photocatalytic degradation
TiO_2 photocatalysis
Advanced oxidation

ABSTRACT

The presence of halogenated organophosphate flame retardants in natural water systems is a widespread concern because of their potential threat to human health and the environment. TiO_2 photocatalysis at 350 nm leads to rapid degradation of tris (2-chloroethyl) phosphate (TCEP). The observed degradation follows pseudo-first-order kinetics at a specific concentration. The apparent rate constants varied from 0.28 to 0.03 min^{-1} depending on the initial concentrations over the range of 18–270 μM, indicating the heterogeneous degradation process is likely controlled by mass transfer (adsorption↔desorption) at the surface of TiO_2. The degradation kinetics also fit the Langmuir-Hinshelwood model with apparent kinetic parameters of 0.03 μM^{-1} and 13.1 μM min^{-1} for the apparent equilibrium constant (K_{LH}) and the reactivity constant ($k_{rxn\text{-}LH}$) respectively. ^{1}H- and ^{31}P-NMR studies indicate sequential oxidation of the alkyl ester chains (alkyl phosphate), initially leading to the diester product, followed by the formation of the monoester and ultimately producing phosphate. Under strongly alkaline conditions the degradation is enhanced, from pH 4 to 9 the degradation is relatively constant, while under highly acidic conditions the degradation is inhibited. Effective mineralization is achieved as demonstrated by excellent chloride (98%) and phosphate (94%) mass balances as well as the loss of total organic carbon (TOC) > 95%. The addition of an equal molar amount of the hydroxyl radical scavenger, coumarin, leads to pronounced reduction in degradation indicating hydroxyl radicals mediate the degradation process. These results demonstrate TiO_2 photocatalytic oxidation has promise for the treatment of aqueous solutions contaminated with organophosphate flame retardants.

1. Introduction

Organophosphorus compounds have been extensively used as pesticides, chemical warfare agents, flame retardants, and plasticizers [1,2]. Organophosphate esters (OPEs), used as flame retardants in a wide range of commercial products including furniture, plastics, automobile, polyurethane foam, and electronic equipment & cable, have attracted significant attention due to their widespread presence in air, water, and sediments [2,3]. OPEs are highly toxic and potential carcinogens from low-level species to high-level vertebrates [4–7]. The growing concerns over human health issues and the adverse effects of OPEs on ecosystems lead to their inclusion in the Toxic Substance Control Act (TSCA) from US EPA [8]. OPEs are additives, not chemically bonded to the host materials, and thus often leach into the surrounding environment [2]. A number of studies detected OPEs in wastewater, drinking water sources, air, dust, and even in biological systems [3,9–12]. Because of their widespread environmental occurrences and documented harmful impacts on human health, treatment of the OPEs has become critical to drinking water providers. Conventional water treatment methods, including activated carbon, membrane filtration, and reverse osmosis are unable to effectively remove OPEs particularly halogenated organophosphate esters [13–16]. The P—O bonds present in the OPEs are generally much more stable to hydrolysis than P—S and P—F bonds present in most pesticides and chemical warfare agents [17]. The stability of the P—O contributes to the relatively long environmental persistence of OPEs.

The TiO_2 photocatalytic degradation of organic compounds has been demonstrated for the destruction of an extensive number of hazardous contaminants in aqueous systems [18,19]. TiO_2 absorbs photons of appropriate wavelengths ($\lambda < 390$ nm) and generates electron (e^-_{CB})/hole (h^+_{VB}) pairs, initiating a series of competing processes represented below in Eqs. (1)–(5). The electron/hole pairs can recombine

* Corresponding author.
E-mail address: osheak@fiu.edu (K.E. O'Shea).

https://doi.org/10.1016/j.jphotochem.2019.03.026
Received 6 December 2018; Received in revised form 13 March 2019; Accepted 18 March 2019
Available online 19 March 2019

or migrate to the surface of TiO_2 and form reactive oxygen species (ROS) in the presence of water and oxygen [20,21].

$$TiO_2 + h\nu \rightarrow h^+_{VB} + e^-_{CB} \quad (1)$$

$$H_2O + h^+_{VB} \rightarrow H^+ + HO^{\cdot} \quad (2)$$

$$O_2 + e^-_{CB} \rightarrow O_2^{\cdot}\text{-} \quad (3)$$

$$\text{Pollutant} + HO^{\cdot} \rightarrow \text{Pollutant}_{OX} \quad (4)$$

$$\text{Pollutant} + h^+_{VB} \rightarrow \text{Pollutant}_{OX} \quad (5)$$

Although a number of reactive oxygen species (ROS) are generated during TiO_2 photocatalysis and can lead to the mineralization of the organic compounds, hydroxyl radicals ($^{\cdot}OH$) are considered the primary species leading to the degradation of organic compounds [22,23]. In general, hydroxyl radicals react with nearly all organic molecules, except per-halogenated or strongly electron deficient compounds. The primary reaction pathways are abstraction (of a hydrogen atom or electron) or addition to an unsaturated π system to yield carbon-centered free radicals. Although less common, electron transfer can also occur from electron rich substrates to $^{\cdot}OH$. The resulting carbon-centered radicals readily react with dissolved molecular oxygen to form organoperoxyl radicals. Subsequent radical chain oxidation processes can ultimately lead to mineralization [24].

A number of reports have appeared on the TiO_2 photocatalysis of organophosphorus compounds [16,25–31]. O'Shea et al. [26] demonstrated rapid TiO_2 photocatalysis of dimethyl methylphosphonate (DMMP) and diethyl methylphosphonate (DEMP). The initial intermediate product resulting from oxidation of alkyl ester chain is a monoester which is subsequently converted to methyl phosphonic acid (MPA) and ultimately phosphate upon continued irradiation. While a number of reaction mechanisms can be envisioned for these transformations, detailed radiolysis studies demonstrated hydroxyl radical initiated hydrogen abstraction from α-hydrogen on ester chain is the primary step in the transformations [32]. There are very few reports on the TiO_2 photocatalytic degradation of halogenated organophosphorus flame retardants. In a recent paper, Antonopoulou et al. [28] reported the TiO_2 photocatalytic degradation of tris (1-chloro-2-propyl) phosphate (TCPP) over the range of 25–500 μg/L using in ultrapure water and real water under solar simulated irradiation. While detailed product studies of the TCPP were not conducted, the diester of TCPP was proposed as an intermediate in route to mineralization. The TiO_2 photocatalysis of TCEP has yet to be reported, however, Ruan et al. demonstrated the degradation of TCEP by UV/H_2O_2 oxidation and proposed its mineralization into Cl^-, PO_4^{3-}, CO_2, and H_2O showing the diester as an intermediate [29]. Cristale et al. [16] reported O_3/UV/H_2O_2 treatment leads to slow degradation and incomplete removal of several halogenated organophosphorus flame retardants from the water. UV/H_2O_2, UV/H_2O_2/O_3, and UV/O_3, mediated degradations of an OPE [30,31] have been reported, however, degradation was dramatically affected by water quality. While advanced oxidation of halogenated OPEs has the potential to produce low molecular weight halogenated aldehydes, ketones and carboxylic acids, analogous to disinfection by-products, detailed product, and mechanistic studies have yet to be reported. We report herein detailed kinetic and product studies for the TiO_2 photocatalysis of TCEP as a model compound of the organophosphate flame retardants.

2. Experimental section

2.1. Materials

Tris (2-chloroethyl) phosphate (TCEP), 2-chloroethanol, and triphenyl phosphate (TPP) were purchased from Aldrich Chemical Company. High purity GC grade dichloromethane (DCM) was obtained from Fisher Scientific. Sodium chloride, sodium hydroxide, nitric acid, sodium carbonate, sodium hydrogen carbonate, potassium dihydrogen phosphate, phosphorus pentoxide, and orthophosphoric acid were also purchased from Fisher Scientific. The catalyst P25 TiO_2 particles [CAS no. 13463-67-7] was supplied by Degussa. Coumarin was purchased from MP Biomedicals, LLC. The oxygen was from Trigas of the highest purity available. Millipore water (18 MΩ cm) and volumetric glassware were used for the preparation of all of the aqueous solutions.

Di (2-chloroethyl) hydrogen phosphate (diester adduct) was synthesized by an alkaline hydrolysis process reported by Barnard et al. [33]. A solution of TCEP (0.21 mol) in 25 mL of 10% NaOH solution was refluxed for 20 h. The reaction mixture was cooled to room temperature, acidified with concentrated hydrochloric acid and the product collected by liquid–liquid solvent extraction with dichloromethane. The yield of product was ~60%. The product was characterized by ^{31}P- & ^{1}H-NMR spectroscopy; ^{31}P-NMR (D_2O, 400 MHz) δ -0.2(1H, q, $^3J_{P\text{-}H}$ = 6.9 Hz), ^{1}H-NMR (D_2O, 400 MHz) δ 4.1(2H, dt, $^3J_{P\text{-}H}$ = 6.8 Hz, $^3J_{H\text{-}H}$ = 5.1 Hz), δ 3.8 (2H, t, $^3J_{H\text{-}H}$ = 5.1 Hz).

2-chloroethyl dihydrogen phosphate (monoester adduct) was prepared by the procedure reported by Via et al. [34]. 2-chloroethanol (12.4 mmoles) was added to phosphorus pentoxide P_2O_5 (6.0 mmoles) and heated for 3 h at nearly 70 °C in presence of 3.3 mmoles of water. After 3 h, the mixture was cooled to room temperature. The yield of monoester measured by ^{31}P-NMR was 65%. NMR details are ^{31}P-NMR (D_2O, 400 MHz) δ -0.52 (1 P, t, $^3J_{P\text{-}H}$ = 7.0 Hz); ^{1}H NMR (D_2O, 400 MHz) δ 3.35 (2H, dt, $^3J_{P\text{-}H}$ = 7.0 Hz, $^3J_{H\text{-}H}$ = 5.4 Hz), 2.92 (2H, t, $^3J_{H\text{-}H}$ = 5.4 Hz).

2.2. Photocatalytic experiment

A Rayonet photochemical reactor equipped with a cooling fan and fourteen phosphor-coated (350 nm) low-pressure black lights in a merry-go-around arrangement was used for all photocatalytic experiments (The details of the photochemical reactor is available at Southern New England Ultra-Violet Company, www.rayonet.org, model RPR-100). The light flux was determined using potassium ferrioxalate actinometry and agreed to within 10% of the manufacturer's specifications (1.6×10^{16} photons/sec/cm^3). A Pyrex glass cylinder vessel with Teflon stopper was used as a reaction vessel (L = 30 cm, D = 2.5 cm). In a typical experiment, a TiO_2 suspension was prepared by adding 10 mg of TiO_2 particles to 100 mL of TCEP aqueous solution. The initial TCEP concentration was varied from 10 to 300 μM for kinetic studies. Higher TCEP concentrations were used for the products studies. The TiO_2 suspensions were sonicated in an ultrasonic cleaning bath for 5 min. to ensure uniform suspension. The suspension was purged with oxygen gently for 10 min prior to irradiation. The aqueous suspension was magnetically stirred and irradiated in the photochemical reactor. The reaction vessel was removed from the reactor at desired time intervals, rigorously shaken for 30 s, then a 5.0 mL aliquot of TiO_2 suspension withdrawn and immediately passed through a 0.45 μm PTFE filter. The filter was rinsed with another 5.0 mL of deionized water and combined with the original filtrate to make the total volume of 10 mL. To investigate the role of solution pH on the TiO_2 photocatalytic degradation of TCEP, NaOH and HNO_3 were added to adjust the corresponding initial pH of aqueous TCEP solution. pH measurements were conducted on Metler Toledo pH meter. For evaluating the contribution of hydroxyl radicals involved in the degradation process, we added coumarin as hydroxyl radical scavenger in TCEP photodegradation.

2.3. GC analysis of TCEP

The concentration of TCEP was monitored by GC (Hewlett-Packard 6890) equipped with an NPD detector. TCEP was extracted from the filtered aqueous solution with dichloromethane (DCM) for analyses. The extraction was carried out in a 40 mL glass extraction vial by adding 5 mL of DCM into 10 mL of aqueous solution. Another 0.075 mL of DCM containing 4000 ppm triphenyl phosphate as an internal

standard was added to each sample. The extraction vial was agitated in an Orbit Shaker (Lab-Line) for 10 min at 300 rpm, before transferring one mL of the DCM phase to a 2.0 mL sample vial for GC analysis. The same extraction procedure was employed in the preparation of calibration standards for the GC NPD. Chromatographic separation was carried out on a DB-5 fused silica capillary column [9]. The sample was injected manually in splitless mode. The injector temperature was set to 250 °C and the detector temperature at 300 °C. The initial GC temperature was held at 40 °C for 4 min. and increased to 190 °C at 15 °C/min and then 10 °C/min to the final temperature of 310 °C which was maintained for 4 min. Helium was used as the carrier gas. The concentration of TCEP was determined using the characteristic retention time, reference standard, careful calibration of NPD detector and quantification using an internal standard. The detector response was calibrated against a series of TCEP aqueous solution ranging from 5 to 300 μM with the internal standard yielding a correlation coefficient (R^2) ≥ 0.99. Standards were run periodically to ensure accurate calibration of GC.

2.4. Analysis of mineralization products

Ion chromatography (IC) was used to monitor phosphate (PO_4^{3-}) and chloride (Cl^-) as mineralization products of TCEP. A 761 Compact IC Metrohm, equipped with a Metrosep A Supp 5 column and conductivity detector was employed using the manufacturer's protocol. A mixture of 3.2 mM sodium carbonate and 1.0 mM sodium hydrogen carbonate aqueous solution was used as a buffer with a flow rate of 0.7 mL/min. The column was regenerated using a 0.125 M solution of sulfuric acid with a flow rate of 2.0 mL/min. The detector response was calibrated, and a standardization curve developed using carefully prepared phosphate from 0.01 to 0.32 mM and chloride from 0.02 to 0.85 mM standard solutions yields correlation coefficients ≥0.99. Total organic carbon (TOC) of irradiated TCEP solution was determined by a TOC-VCSH analyzer (Shimadzu, Japan) using a high-temperature platinum combustion method [35]. An aliquot of twenty mL of irradiated TCEP solution was filtered, then acidified to pH < 2 with 3 N HCl and sparged with CO_2-free compressed air before injection. The combustion derived CO_2 was carried by ultra-zero grade compressed air and detected by a non-dispersive infrared CO_2 detector.

2.5. Analysis of intermediates and byproducts

An NMR spectrometer (Bruker-Spectrospin 400 Ultrashield) was used to record the ^{31}P-NMR (162 MHz) and ^{1}H NMR (400 MHz) spectra of starting materials and to monitor intermediate and final products during the TiO_2 photocatalysis of TCEP [36]. The ^{31}P-NMR chemical shifts were reported in ppm with respect to the resonance peak of 85% H_3PO_4 used as an external chemical shift reference. For the NMR product studies, the initial concentration of TCEP was 15.06 mM.

3. Results and discussion

3.1. Photocatalytic degradation

Photocatalysis of TCEP (109 μM) at 350 nm in an O_2-saturated aqueous suspension of TiO_2 leads to rapid degradation, shown in Fig. 1. Control experiments run in the absence of TiO_2 or light demonstrated that direct photolysis and hydrolysis and/or adsorption of TCEP was insignificant. However, under photocatalytic conditions (TiO_2/hv/O_2), more than 50% of TCEP was eliminated within 10 min of irradiation, as shown in Fig. 1. The observed rate of TCEP degradation decreased with the time of irradiation. The reduction in the rate of degradation as a function of treatment time is attributed to lower TCEP concentrations and the increase of by-product concentrations competing with TCEP for active sites at the surface of TiO_2 [26,28]. Complete degradation of TCEP was observed within 60 min of irradiation.

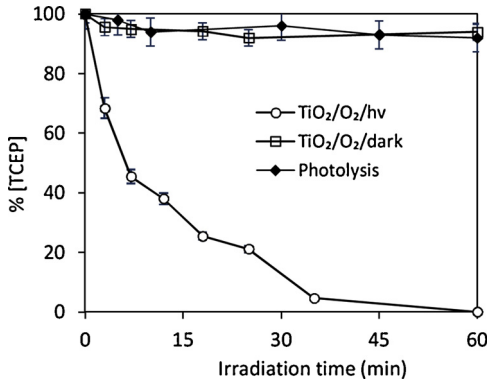

Fig. 1. TiO_2 photocatalysis of TCEP at 350 nm in O_2-saturated suspension; $[TCEP]_0$ = 109 μM; $[TiO_2]$ = 0.10 g/L and pH = 6.5. The reproducibility was within 5% based on representative triplicate runs.

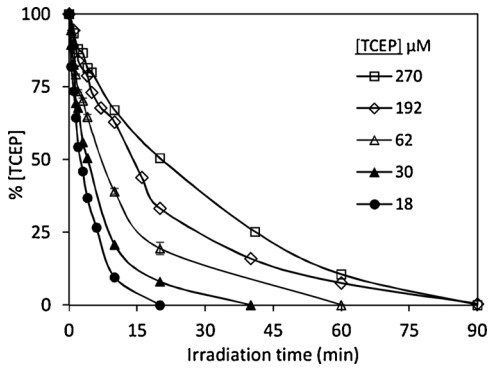

Fig. 2. Degradation kinetics of TCEP ($[TCEP]_0$ = 18–270 μM) upon irradiation at 350 nm at O_2-saturated TiO_2 (0.10 g/L) aqueous suspension.

The degradation kinetics of TCEP were studied over a range of initial concentrations from 18 to 270 μM, shown in Fig. 2. The initial degradation rates of TCEP as a function of starting substrate concentration were determined from the first 15–20% disappearance of the TCEP to minimize the effect of products on the initial kinetic parameters and summarized in Table 1.

With increasing initial TCEP concentration the observed degradation rate decreases. This observation is rationalized based on the finite number of reactive sites on the TiO_2 surface or adsorbed $^{\cdot}OH$ thus as the initial TCEP concentration increases, the portion of adsorbed target compounds on the TiO_2 surface compared to those in solution decreases reducing the observed rate. In addition, the by-products of TCEP may slow down the degradation because of competition for adsorption sites and hydroxyl radicals [28]. Plots of pseudo-first-order kinetics for the TiO_2 photocatalytic degradation of TCEP are presented in Fig. 3. The rate constants (k) were calculated from the slope of the linear pseudo-first-order equation, $[\ln C_t/C_0 = -kt]$ where C_t and C_0 are the concentrations of TCEP at time t and at the start of the reaction. The results

Table 1
Initial degradation rates and their corresponding pseudo-first-order rate constant of TCEP as a function of concentration by TiO_2 photocatalytic oxidation in O_2-saturated aqueous solution.

[TCEP] (μM)	Initial rate (μMmin^{-1})	R^2 value for initial rate	Pseudo-first-order rate constant (min^{-1})	R^2 value for rate constant
18	4.4	0.96	0.28	0.96
30	5.9	0.95	0.19	0.97
62	8.0	0.96	0.12	0.95
192	10.6	0.95	0.05	0.98
270	12.2	0.93	0.03	0.99

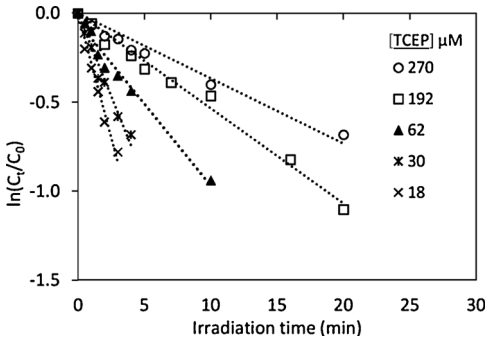

Fig. 3. Pseudo-first-order kinetics plots of TCEP degradation upon irradiation at 350 nm in O_2-saturated TiO_2 (0.10 g/L) aqueous suspension.

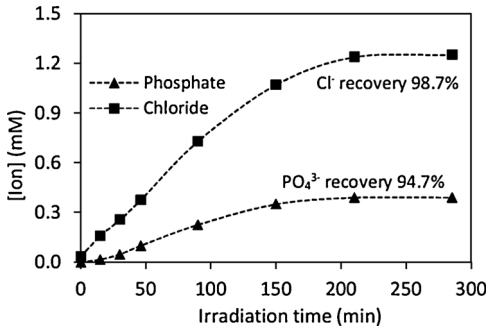

Fig. 5. Evolution of PO_4^{3-} and Cl^- ion upon irradiation at 350 nm in O_2-saturated TiO_2 aqueous suspension; $[TCEP]_0$ = 0.422 mM, $[TiO_2]$ = 0.10 g/l; reproducible ± 5% based on a representative triplicate runs.

are summarized in Table 1. While the results for a given concentration of TCEP are consistent with pseudo-first-order kinetics, by the virtue of the linear relationship of $\ln(C_t/C_0)$ as function of time, the change in the rate constant as a function of initial concentration suggests that the reaction kinetics are more complex than a simple first order reaction. The observed rate constant increases by an order of magnitude when the substrate concentration is decreased by nearly 15 fold. Similarly, a reduction of the reaction order as a function of substrate concentration in the TiO_2 photocatalysis have been reported by Sabin et al. [37]. The change in the rate constant can be the result of mass transfer limitations (adsorption↔desorption) at the surface of TiO_2.

TiO_2 photocatalysis is a heterogeneous process requiring adsorption and reaction at or near the surface of TiO_2 [20,38,39]. The Langmuir-Hinshelwood (L-H) kinetic model has been effectively employed in the modeling of TiO_2 photocatalytic transformation to an extensive number of organics by plotting the initial degradation rates as a function of concentration [19,40,41]. The L-H equation is represented in Eq. (6) where r_0 is initial degradation rate of target materials, C_0 is the initial concentration of substrate, $k_{rxn\text{-}LH}$ is the reactivity constant, and K_{LH} is the apparent equilibrium constant.

$$\textit{Langmuir} - \textit{Hinshelwood equation}: \quad {}^{1}/_{r_0} = {}^{1}/_{k_{rxn-LH} K_{LH} C_0} + {}^{1}/_{k_{rxn-LH}} \tag{6}$$

The L-H experiment was conducted over a range of initial concentrations (18–270 µM) at constant TiO_2 concentration under uniform light intensity. Based on the value of the least-square fit correlation coefficient ($R^2 \geq 0.988$) of the L-H plot, Fig. 4, the degradation kinetics of TCEP is in good agreement with the Langmuir-Hinshelwood mechanism. The L-H kinetic parameters determined from the slope and intercept of the L-H plot are $K_{LH} = 0.03\ \mu M^{-1}$ and $k_{rxn\text{-}LH} = 13.1\ \mu M\ min^{-1}$. The L-H kinetic parameters are often referred to as apparent kinetic parameters which may not correlate to their original intended kinetic parameters [42]. However, the L-H kinetic parameters are valuable for predicting degradation rates and for making comparisons among different compounds over a range of reaction conditions [43]. The equilibrium constant, K_{LH}, is theoretically associated to the partitioning of TCEP at the surface of TiO_2 and $k_{rxn\text{-}LH}$ is a coefficient related to the reactivity of the target compounds (susceptibility of TCEP to degradation). TiO_2 photocatalytic induced degradation of TCEP adheres to pseudo-first-order and the L-H kinetic models despite the complex interplay among the production of hydroxyl radicals at the surface and the surface adsorption↔desorption of target compounds leading to the degradation.

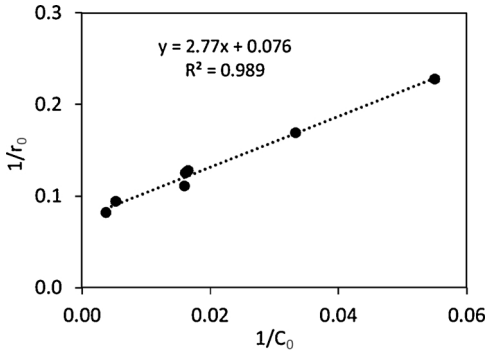

Fig. 4. Langmuir-Hinshelwood plot of TiO_2 photodegradation of TCEP ($[TCEP]_0$ = 18–270 µM) upon irradiation at 350 nm at O_2-saturated TiO_2 (0.10 g/L) aqueous suspension.

3.2. Mineralization of TCEP

The TiO_2 photocatalytic mineralization of TCEP was assessed by measuring the production of PO_4^{3-} and Cl^-, Fig. 5, as well as the total organic carbon (TOC) present in solution, Fig. 6, as a function of irradiation time. Excellent phosphate and chloride mass balances were observed upon extended irradiation. TCEP contains one phosphorus atom and three chlorine atoms. From an initial concentration of 0.422 mM of TCEP, 0.40 mM of phosphate (94.7%) and 1.25 mM of chloride (98.7%) ions were measured by IC. While Antonopoulou et al. reported an almost complete mass balance of chloride ions, a phosphorus mass balance of only 60% was reported during the TiO_2 photocatalytic degradation of TCPP [28]. We observed TiO_2 photocatalysis of TCEP was complete within an hour, however, to achieve extensive transformation of TCEP and by-products to phosphate required extended irradiation. The delay in phosphate mass balance indicates the involvement of intermediate products [44,45]. The starting material, TCEP, is degraded within 50 min at which time the mass balances for chloride is 35% and for phosphate 25%. Once the TCEP is fully degraded the formation of chloride and phosphate continues for another ~2 h of treatment. After ~3 h of irradiation mineralization to chloride

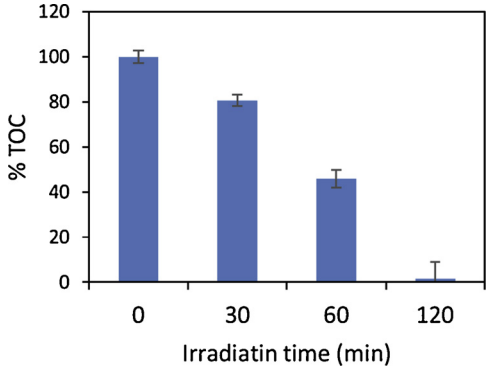

Fig. 6. Reduction of total organic carbon (TOC) as a function of the irradiation time of TiO_2 photocatalysis of TCEP; $[TCEP]_0$ = 110 µM, $[TiO_2]$ = 0.10 g/L; data is reproducible nearly 5% standard deviation.

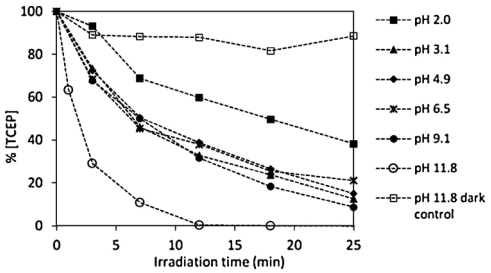

Fig. 7. TiO_2 photodegradation of TCEP in O_2-saturated aqueous suspension at 350 nm irradiation over a range of solution pH ($[TCEP]_0$ = 109 μM, $[TiO_2]$ = 0.10 g/L).

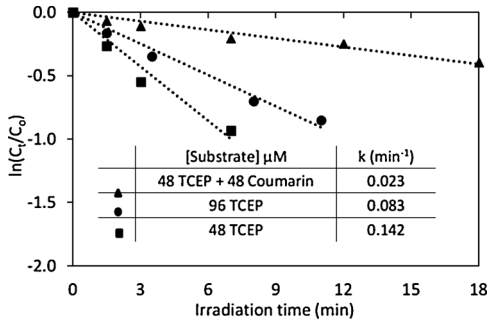

Fig. 8. Effect of coumarin on the degradation of TCEP in O_2 saturated TiO_2 suspension at 350 nm.

and phosphate is ≥95%. The delay in the formation of mineralization products relative to the disappearance of TCEP indicates the presence of chlorinated organic by-products with and without phosphorus at longer treatment times.

Mineralization of TCEP by TiO_2 photocatalytic irradiation is further supported by the monitoring of the level of TOC in the reaction solution. The initial [TCEP] was 110 μM for TOC measurements in an aqueous solution irradiated over TiO_2 photocatalyst. Results demonstrate that ~50% of TOC was removed from the reaction solution within one hour. Over the 2 h of irradiation, more than 95% TOC removal indicating near complete mineralization.

3.3. Effect of solution pH on TiO_2 photodegradation of TCEP

Solution pH can have a pronounced effect on the TiO_2 photocatalytic degradation of organophosphorus compounds [17,46]. The effect of solution pH on photocatalytic degradation of TCEP was evaluated by varying the solution pH from highly acidic (pH 2.0) to highly alkaline (pH 11.8) conditions, illustrated in Fig. 7. At modestly acidic to basic conditions (pH 4–9), the rates of degradation are relatively constant. However, under highly acidic pH the rate of TCEP degradation decreases while under highly basic pH the rate of degradation increases significantly. Since the phosphate ester functional group can undergo base hydrolysis, a dark control experiment at the highly alkaline pH was carried out. However, no significant loss of TCEP was observed under highly alkaline conditions in the dark. A number of factors can contribute to the enhanced photocatalytic degradation at alkaline conditions. The surface of TiO_2 under alkaline conditions has negative charge which can lead to reduced agglomeration compared to neutral conditions. Reduced agglomeration can contribute to higher surface area, higher adsorption and faster degradation rates [47]. In addition, at high pH the surface of TiO_2 is negative, and thus the probability of adsorption of anionic by-products and phosphate decreases leading to the faster degradation of a neutral target compound. The pKa of the hydroxyl radical is 11.5. Thus at pH 11.8, hydroxyl radical is converted to an oxygen atom radical anion ($^{\cdot}OH \rightleftharpoons O^{\cdot -} + H^+$) which may have higher reactivity [48].

3.4. Scavenging studies to assess the contribution of hydroxyl radicals

While hydroxyl radicals are often considered the predominant species initiating the degradation processes during TiO_2 photocatalysis, other species can also contribute to the degradation. The reactions of hydroxyl radicals with organic compounds is a bimolecular process [30,49,50]. To probe the role of hydroxyl radical, coumarin, a well-known hydroxyl radical trap was added to the reaction solution [51]. Upon addition of an equimolar amount of coumarin, the degradation decreases by ~70%, which indicates hydroxyl radicals are the main species participating in the degradation process of TCEP, illustrated in Fig. 8.

The second order rate constant (k) of hydroxyl radical for coumarin is $k_{\cdot OH+COU} = 2.9 \times 10^9$ $M^{-1}s^{-1}$ and for TCEP is $k_{\cdot OH+TCEP} = 5.6 \times 10^8$ $M^{-1}s^{-1}$ [30], the ~70–75% reduction of TCEP degradation with the addition of coumarin is nicely correlated to competition kinetics for hydroxyl radical. The observed rate for TCEP degradation decreases ~70–75 % from 0.083 to 0.023 min^{-1} upon the addition of an equimolar amount of scavenger. A ~50% decrease in the reaction rate for TCEP degradation would be expected if the rate constants were equal. The 75% decrease observed reflects the faster bimolecular rate constant for coumarin being almost double the rate constant, (2.9/5.6 ~ 52%) for the reaction of TCEP with $^{\cdot}OH$. Thus diluting the relative concentration of TCEP by 50% decreases rate by 50% and since the bimolecular hydroxyl radical rate constant for TCEP is 52% of the rate constant for coumarin the overall theoretical rate decreases to 0.50 × 0.52 = 0.26 or 26%. Normalization of the original observed rate for the dilution and difference in reactivity gives a theoretical rate 0.083 min^{-1} x 0.26 = 0.22 min^{-1} which is within the experimental error of the observed rate 0.23 min^{-1} indicating that hydroxyl radical is the predominant species leading to the degradation of TCEP under our experimental conditions.

3.5. Products studies

Product studies are critical to establish the course of degradation and to determine the formation and fate of intermediates during the TiO_2 photocatalytic degradation. The halogenated organophosphate esters are composed of carbon, hydrogen, oxygen, phosphorus, and halogen atoms. The final mineralized degradation products of TCEP are CO_2, H_2O, phosphate (PO_4^{3-}), and chloride (Cl^-) ions. As discussed earlier, the TiO_2 photocatalytic degradation of TCEP yields near the stoichiometric amount of chloride and phosphate ions as mineralization products (Scheme 1), but intermediates products have yet to be reported. Based on previous studies of organophosphorus compounds, oxidation of alkyl phosphate ester groups can be achieved by TiO_2 photocatalysis, thus subsequent conversion of TCEP to the diester adduct, TCEP-diester subsequently to the TCEP-monoester is proposed as shown in scheme 1 [17]. Mass spectrometry (MS) is a powerful tool and has been extensively used for identifying oxidative products in TiO_2 photocatalysis. MS identification is based primarily on molecular weight and often cannot distinguish among constitutional and geometric isomers. In addition, an elevated capillary temperature is used in MS during the ionization which may lead to a potential transformation of products generated during photocatalytic oxidation. With this in

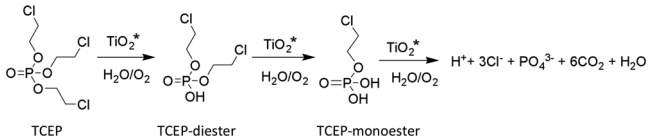

Scheme 1. Reaction pathways for TiO_2 photocatalytic degradation of TCEP to mineralization products (TiO_2* indicates photoactivation).

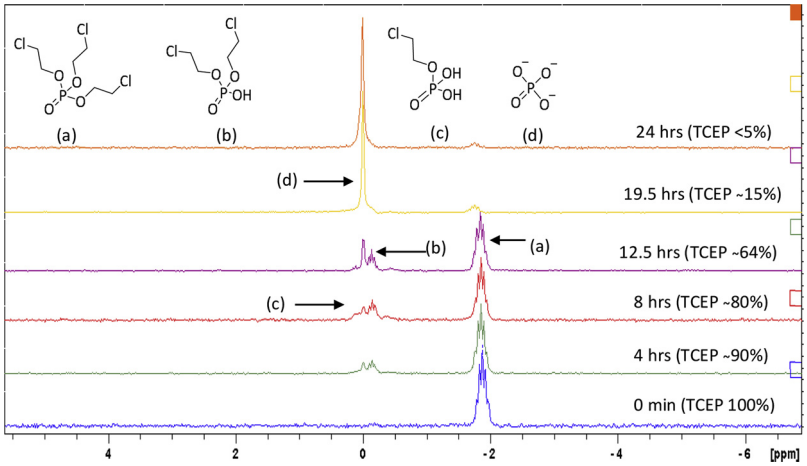

Fig. 9. ^{31}P-NMR spectrum of TiO_2 photodegradation of TCEP ($[TCEP]_0$ = 15.06 mM).

mind, NMR spectrometry allows for detailed characterization of the products at room temperature during TiO_2 photocatalysis of TCEP. To identify and monitor the phosphorus-containing intermediate products during photocatalysis, the ^{31}P-NMR spectra of TCEP reaction mixtures were recorded as a function of treatment time, illustrated in Fig. 9.

We identified di(2-chloroethyl) hydrogen phosphate (TCEP-diester) as the main phosphorus-containing intermediate during the photocatalysis. The identity of this intermediate was confirmed by ^{31}P-NMR and ^{1}H-NMR via comparison with our prepared authentic samples. Complete mineralization of TCEP into phosphate ions was also confirmed by NMR studies comparing the signal of the ^{31}P-NMR spectrum of phosphoric acid. Previous reports established that phosphonates are transformed from diester to monoester via oxidation of ester side chain and finally mineralized to phosphates [17], and in this study, monoester of TCEP, 2-chloroethyl dihydrogen phosphate (TCEP-monoester), was also identified. ^{1}H-NMR characterization of the reaction solutions did not indicate the presence of detectable amounts of chloroacetic acid, chloroacetaldehyde, 2-chloroethanol. The production and lifetime of low molecular weight organochlorine compounds appear to be short given the excellent Cl^- mass balance upon continued irradiation. Ruan et al. [29] proposed ester type intermediates in the degradation of TCEP by UV/H_2O_2. However, they only identified small organic molecules like formic acid, acetic acid, and phosphate in PO_4^{3-} without reporting any organophosphorus or organochlorine by-products. The time profile for the disappearance of TCEP and the formation of diester, monoester and phosphate products during the photocatalysis is illustrated in Fig. 10.

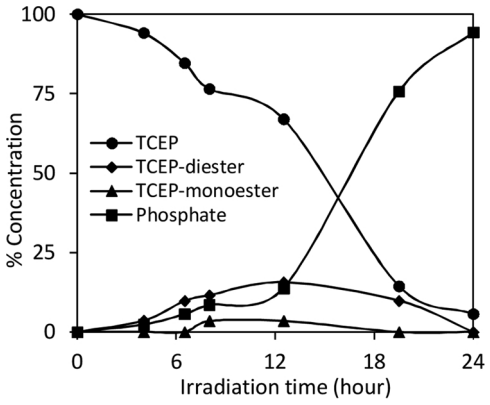

Fig. 10. The phosphorus-containing products distribution during TiO_2 photocatalysis of TCEP ($[TCEP]_0$ = 15.06 mM) in D_2O solution monitored by ^{31}P-NMR.

4. Mechanistic consideration

A number of reaction mechanisms can be envisioned to explain the formation of major diester type compound of TCEP. Hydroxyl radical (˙OH) reacts with organic molecule via one of the three different mechanisms: hydrogen atom abstraction, electrophilic addition to the double bond, and electron transfer from an organic molecule. Based on these insights and detailed mechanistic studies of related organophosphates, probable mechanisms for the hydroxyl radical-mediated conversion of TCEP into its diester, monoesters and finally to mineralization are shown in scheme 2 involving hydrogen abstraction mechanism.

In this mechanism, a hydrogen atom is abstracted from ethyl ester carbon leading to the formation of a carbon-centered radical. The hydrogens alpha to the oxygen atom and chlorine atom will be activated towards abstraction by electronic effects, but the more reactive position should be alpha to the oxygen atom. The resulting carbon-centered radical can undergo further oxidation leading to the formation of an acetal, either by direct reaction with another hydroxyl radical, which in aqueous solution will be converted to the partially hydrolyzed ester or by the addition of oxygen to form a peroxyl radical. The dimerization of two peroxyl radicals followed by extrusion of O_2 via a Russell mechanism can also be used to explain the observed products [17]. Oxidation of the remaining 2-chloroethoxy group yields 2-chloroethyl dihydrogen phosphate. Subsequent hydroxyl radical-mediated oxidation can convert the diester adduct to monoester adduct and subsequently to phosphate. The formation of di (2-chloroethyl) hydrogen phosphate and 2-chloroethyl dihydrogen phosphates are consistent with the hydroxyl radical-mediated pathways, even though the 2-chloroethyl-dihydrogen phosphate disappears quickly. This may be due to the hydroxyl radicals readily oxidizing the 2-chloroethyl-dihydrogen phosphate at the surface of the photocatalyst and finally mineralization to phosphate ion.

5. Conclusions

We have shown the TiO_2 photocatalytic degradation of the organophosphate flame retardant, tris (2-chloroethyl) phosphate (TCEP), is effective upon the irradiation at 350 nm in oxygen-saturated aqueous suspension. The degradation follows pseudo-first-order kinetics with varying rate constant depending on the initial concentration of TCEP and fits to Langmuir-Hinshelwood model. The apparent kinetic parameters obtained from the application of these models can be used for predictive purposes and to address treatment objectives. Intermediate products included the di- and mono-esters adducts which were conclusively identified by comparison with authentic samples using ^{1}H- and ^{31}P-NMR. Final products from extended irradiation demonstrate

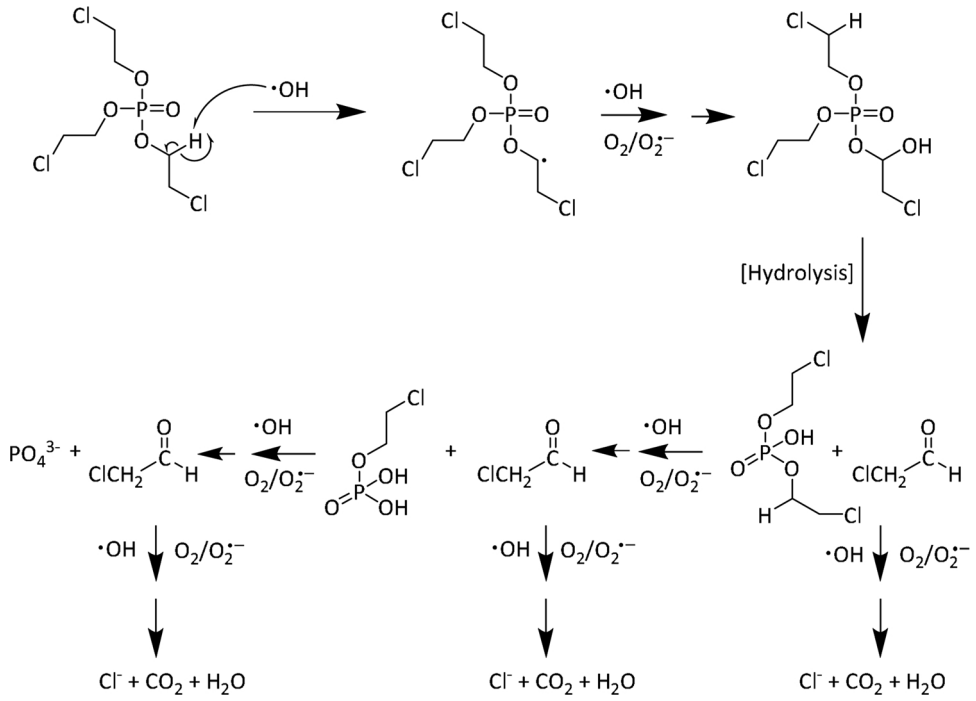

Scheme 2. Proposed hydroxyl radical-mediated degradation mechanism of TCEP.

nearly complete mineralization can be obtained upon extended treatment. Mechanistic consideration indicates the degradation proceeds via hydroxyl radical-mediated pathways. These results suggest that TiO_2 photocatalytic oxidation will be useful for the decontamination of aqueous solutions contaminated with the recalcitrant organophosphate compounds.

Acknowledgement

We acknowledge partial support from National Science Foundation under award number CHE-1710111.

References

[1] Y.C. Yang, J.A. Baker, J.R. Ward, Decontamination of chemical warfare agents, Chem. Rev. 92 (1992) 1729–1743.
[2] I. van der Veen, J. de Boer, Phosphorus flame retardants: properties, production, environmental occurrence, toxicity and analysis, Chemosphere 88 (2012) 1119–1153, https://doi.org/10.1016/j.chemosphere.2012.03.067.
[3] G.L. Wei, D.Q. Li, M.N. Zhuo, Y.S. Liao, Z.Y. Xie, T.L. Guo, J.J. Li, S.Y. Zhang, Z.Q. Liang, Organophosphorus flame retardants and plasticizers: sources, occurrence, toxicity, and human exposure, Environ. Pollut. 196 (2015) 29–46, https://doi.org/10.1016/j.envpol.2014.09.012.
[4] D. Crump, S. Chiu, S.W. Kennedy, Effects of tris (1,3-dichloro-2-propyl) phosphate and tris (1-chloropropyl) phosphate on cytotoxicity and mRNA expression in primary cultures of avian hepatocytes and neuronal cells, Toxicol. Sci. 126 (2012) 140–148, https://doi.org/10.1093/toxsci/kfs015.
[5] J. Li, J.P. Giesy, L. Yu, G. Li, C. Liu, Effects of tris (1,3-dichloro-2- propyl) phosphate (TDCPP) in Tetrahymena thermophila: targeting the ribosome, Nat. Publ. Gr. (2015) 1–9, https://doi.org/10.1038/srep10562.
[6] J.D. Meeker, E.M. Cooper, H.M. Stapleton, R. Hauser, Urinary metabolites of organophosphate flame retardants: temporal variability and correlations with house dust concentrations, Environ. Health Perspect. 121 (2013) 580–585, https://doi.org/10.1289/ehp.1205907.
[7] P.J. Morris, D. Medina-Cleghorn, A. Heslin, S.M. King, J. Orr, M.M. Mulvihill, R.M. Krauss, D.K. Nomura, Organophosphorus flame retardants inhibit specific liver carboxylesterases and cause serum hypertriglyceridemia, ACS Chem. Biol. 9 (2014) 1097–1103, https://doi.org/10.1021/cb500014r.
[8] E.D. Schreder, M.J. La Guardia, Flame retardant transfers from U.S. households (dust and laundry wastewater) to the aquatic environment, Environ. Sci. Technol. 48 (2014) 11575–11583, https://doi.org/10.1021/es502227h.
[9] A. Marklund, B. Andersson, P. Haglund, Organophosphorus flame retardants and plasticizers in Swedish sewage treatment plants, Environ. Sci. Technol. 39 (2005) 7423–7429, https://doi.org/10.1021/es0510131.
[10] J. Cristale, A. García Vázquez, C. Barata, S. Lacorte, Priority and emerging flame retardants in rivers: occurrence in water and sediment, daphnia magna toxicity and risk assessment, Environ. Int. 59 (2013) 232–243, https://doi.org/10.1016/j.envint.2013.06.011.
[11] A. Araki, I. Saito, A. Kanazawa, K. Morimoto, K. Nakayama, E. Shibata, M. Tanaka, T. Takigawa, T. Yoshimura, H. Chikara, Y. Saijo, R. Kishi, Phosphorus flame retardants in indoor dust and their relation to asthma and allergies of inhabitants, Indoor Air 24 (2014) 3–15, https://doi.org/10.1111/ina.12054.
[12] E. Martínez-Carballo, C. González-Barreiro, A. Sitka, S. Scharf, O. Gans, Determination of selected organophosphate esters in the aquatic environment of Austria, Sci. Total Environ. 388 (2007) 290–299, https://doi.org/10.1016/J.SCITOTENV.2007.08.005.
[13] M. Garcia-Lopez, I. Rodriguez, R. Cela, Development of a dispersive liquid-liquid microextraction method for organophosphorus flame retardants and plastizicers determination in water samples, J. Chromatogr. A 1166 (2007) 9–15, https://doi.org/10.1016/j.chroma.2007.08.006.
[14] S.D. Kim, J. Cho, I.S. Kim, B.J. Vanderford, S.A. Snyder, Occurrence and removal of pharmaceuticals and endocrine disruptors in South Korean surface, drinking, and waste waters, Water Res. 41 (2007) 1013–1021, https://doi.org/10.1016/j.watres.2006.06.034.
[15] P.E. Stackelberg, J. Gibs, E.T. Furlong, M.T. Meyer, S.D. Zaugg, R.L. Lippincott, Efficiency of conventional drinking-water-treatment processes in removal of pharmaceuticals and other organic compounds, Sci. Total Environ. 377 (2007) 255–272, https://doi.org/10.1016/j.scitotenv.2007.01.095.
[16] J. Cristale, D.D. Ramos, R.F. Dantas, A. Machulek Junior, S. Lacorte, C. Sans, S. Esplugas, Can activated sludge treatments and advanced oxidation processes remove organophosphorus flame retardants? Environ. Res. 144 (2016) 11–18, https://doi.org/10.1016/j.envres.2015.10.008.
[17] K.E. O'Shea, Titanium dioxide-photocatalyzed reactions of organophosphorus compounds in aqueous media, Semicond. Photochem. Photophysics (2003) 231–247.
[18] N. Serpone, Brief introductory remarks on heterogeneous photocatalysis, Sol. Energy Mater. Sol. Cells 38 (1995) 369–379, https://doi.org/10.1016/0927-0248(94)00230-4.
[19] D.F. Ollis, E. Pelizzetti, N. Serpone, Photocatalyzed destruction of water contaminants, Environ. Sci. Technol. 25 (1991) 1522–1529, https://doi.org/10.1021/es00021a001.
[20] M.R. Hoffmann, S. Martin, W. Choi, D.W. Bahnemann, Environmental applications of semiconductor photocatalysis, Chem. Rev. 95 (1995) 69–96, https://doi.org/10.1021/cr00033a004.
[21] M. Pelaez, N.T. Nolan, S.C. Pillai, M.K. Seery, P. Falaras, A.G. Kontos, P.S.M. Dunlop, J.W.J. Hamilton, J.A. Byrne, K. O'Shea, M.H. Entezari, D.D. Dionysiou, A review on the visible light active titanium dioxide photocatalysts for environmental applications, Appl. Catal. B: Environ. 125 (2012) 331–349, https://doi.org/10.1016/j.apcatb.2012.05.036.
[22] H. Al-Ekabi, N. Serpone, E. Pelizzetti, C. Minero, M.A. Fox, R.B. Draper, Kinetic studies in heterogeneous photocatalysis. 2. TiO_2-mediated degradation of 4-chlorophenol alone and in a three-component mixture of 4-chlorophenol, 2,4-dichlorophenol, and 2,4,5-trichlorophenol in air-equilibrated aqueous media, Langmuir 5 (1989) 250–255, https://doi.org/10.1021/la00085a048.
[23] K. Ishibashi, A. Fujishima, T. Watanabe, K. Hashimoto, Quantum yields of active

oxidative species formed on TiO_2 photocatalyst, J. Photochem. Photobiol. A: Chem. 134 (2000) 139–142.
[24] W.J. Cooper, C.J. Cramer, N.H. Martin, S.P. Mezyk, K.E. O'Shea, C. von Sonntag, Free radical mechanisms for the treatment of methyl tert-butyl ether (MTBE) via advanced oxidation/reductive processes in aqueous solutions, Chem. Rev. 109 (2009) 1302–1345.
[25] K.E. O'Shea, I. Garcia, M. Aguilar, TiO_2 photocatalytic degradation of dimethyl- and diethyl- methylphosphonate, effects of catalyst and environmental factors, Res. Chem. Intermed. 23 (1997) 325–339, https://doi.org/10.1163/156856797X00556.
[26] K.E. O'Shea, S. Beightol, I. Garcia, M. Aguilar, D.V. Kalen, W.J. Cooper, Photocatalytic decomposition of organophosphonates in irradiated TiO_2 suspensions, J. Photochem. Photobiol. A: Chem. 107 (1997) 221–226, https://doi.org/10.1016/S1010-6030(96)04420-6.
[27] K.E. O'Shea, Ailette Aguila, K. Vinodgopal, Prashant V. Kamat, Reaction pathways and kinetics parameters of sonolytically induced oxidation of dimethyl methylphosphonate in air saturated aqueous solutions, Res. Chem. Intermed. 24 (1998) 695–705.
[28] M. Antonopoulou, P. Karagianni, I.K. Konstantinou, Kinetic and mechanistic study of photocatalytic degradation of flame retardant tris (1-chloro-2-propyl) phosphate (TCPP), Appl. Catal. B: Environ. 192 (2016) 152–160, https://doi.org/10.1016/j.apcatb.2016.03.039.
[29] X.-C. Ruan, X. Jin, Z.-Y. Yang, Q.-F. Zeng, Photodegradation of tris (2-chloroethyl) phosphate in aqueous solution by UV/O_3, Water Air Soil Pollut. Focus 224 (2013) 1405–1414, https://doi.org/10.1007/s11270-014-2085-8.
[30] M.J. Watts, K.G. Linden, Advanced oxidation kinetics of aqueous trialkyl phosphate flame retardants and plasticizers, Environ. Sci. Technol. 43 (2009) 2937–2942, https://doi.org/10.1021/es8031659.
[31] X. Yuan, S. Lacorte, J. Cristale, R.F. Dantas, C. Sans, S. Esplugas, Z. Qiang, Removal of organophosphate esters from municipal secondary effluent by ozone and UV/H_2O_2 treatments, Sep. Purif. Technol. 156 (2015) 1028–1034, https://doi.org/10.1016/j.seppur.2015.09.052.
[32] A. Aguila, K.E. O'Shea, T. Tobien, K.D. Asmus, Reactions of hydroxyl radical with dimethyl methylphosphonate and diethyl methylphosphonate. A fundamental mechanistic study, J. Phys. Chem. A 105 (2001) 7834–7839, https://doi.org/10.1021/jp002367w.
[33] P.W.C. Barnard, C.A. Bunton, D.R. Llewellyn, C.A. Vernon, V.A. Welch, The reactions of organic phosphates. Part V. The hydrolysis of triphenyl and trimethyl phosphates, J. Chem. Soc. 0 (1961) 2670, https://doi.org/10.1039/jr9610002670.
[34] F.S. Via, S.Y. Liu, Synthesis of mono-alkyl acid phosphates with high mono-content, US Pat. 4126650. (1978).
[35] Y. Ding, K.M. Cawley, C.N. da Cunha, R. Jaffé, Environmental dynamics of dissolved black carbon in wetlands, Biogeochemistry (2014), https://doi.org/10.1007/s10533-014-9964-3.
[36] F. Benoit-Marquié, C. de Montety, V. Gilard, R. Martino, M.T. Maurette, M. Malet-Martino, Dichlorvos degradation studied by ^{31}P-NMR, Environ. Chem. Lett. 2 (2004) 93–97, https://doi.org/10.1007/s10311-004-0076-5.
[37] F. Sabin, T. Türk, A. Vogler, Photo-oxidation of organic compound in the presence of titanium dioxide: determination of the efficiency, J. Photochem. Photobiol. A: Chem. 63 (1992) 99–106, https://doi.org/10.1016/1010-6030(92)85157-P.
[38] E. Pelizzetti, Concluding remarks on heterogeneous solar photocatalysis, Sol. Energy Mater. Sol. Cells 38 (1995) 453–457, https://doi.org/10.1016/0927-0248(94)00237-1.
[39] C. Minero, F. Catozzo, E. Pelizzetti, Role of adsorption in photocatalyzed reactions of organic-molecules in aqueous TiO_2 suspensions, Langmuir 8 (1992) 481–486, https://doi.org/10.1021/la00038a029.
[40] W. Adamson, P. Gast, Physical Chemistry of Surfaces, Sixth Edition, (1997), https://doi.org/10.1149/1.2133374.
[41] H. Al-Ekabi, N. Serpone, Kinetics studies in heterogeneous photocatalysis. I. Photocatalytic degradation of chlorinated phenols in aerated aqueous solutions over titania supported on a glass matrix, J. Phys. Chem. 92 (1988) 5726–5731, https://doi.org/10.1021/j100331a036.
[42] S. Azizian, S. Eris, L.D. Wilson, Re-evaluation of the century-old Langmuir isotherm for modeling adsorption phenomena in solution, Chem. Phys. 513 (2018) 99–104, https://doi.org/10.1016/j.chemphys.2018.06.022.
[43] K.E. O'Shea, C. Cardona, Hammett study on the TiO_2-catalyzed photooxidation of para-substituted phenols. A kinetic and mechanistic analysis, J. Org. Chem. 59 (1994) 5005–5009, https://doi.org/10.1021/jo00096a052.
[44] T. Oncescu, M.I. Stefan, P. Oancea, Photocatalytic degradation of dichlorvos in aqueous TiO_2 suspensions, Environ. Sci. Pollut. Res. 17 (2010) 1158–1166, https://doi.org/10.1007/s11356-009-0292-4.
[45] E. Evgenidou, I. Konstantinou, K. Fytianos, T. Albanis, Study of the removal of dichlorvos and dimethoate in a titanium dioxide mediated photocatalytic process through the examination of intermediates and the reaction mechanism, J. Hazard. Mater. 137 (2006) 1056–1064, https://doi.org/10.1016/j.jhazmat.2006.03.042.
[46] U.I. Gaya, A.H. Abdullah, Heterogeneous photocatalytic degradation of organic contaminants over titanium dioxide: a review of fundamentals, progress and problems, J. Photochem. Photobiol. C: Photochem. Rev. 9 (2008) 1–12, https://doi.org/10.1016/j.jphotochemrev.2007.12.003.
[47] K.E. O'Shea, E. Pernas, J. Saiers, Influence of mineralization products on the coagulation of TiO_2 photocatalyst, Langmuir 15 (1999) 2071–2076, https://doi.org/10.1021/la9806808.
[48] G.A. Poskrebyshev, P. Neta, R.E. Huie, Temperature dependence of the acid dissociation constant of the hydroxyl radical, J. Phys. Chem. A 106 (2002), https://doi.org/10.1021/jp020239x.
[49] G.V. Buxton, C.L. Greenstock, W.P. Helman, A.B. Ross, Critical review of rate constants for reactions of hydrated electrons, hydrogen atoms and hydroxyl radicals (OH/O) in aqueous solution, J. Phys. Chem. Ref. Data 17 (1988) 513–886, https://doi.org/10.1063/1.555805.
[50] S. Schnell, C. Mendoza, The condition for pseudo-first-order kinetics in enzymatic reactions is independent of the initial enzyme concentration, Biophys. Chem. 107 (2004) 165–174, https://doi.org/10.1016/j.bpc.2003.09.003.
[51] H. Czili, A. Horváth, Applicability of coumarin for detecting and measuring hydroxyl radicals generated by photoexcitation of TiO_2 nanoparticles, Appl. Catal. B: Environ. 81 (2008) 295–302, https://doi.org/10.1016/j.apcatb.2008.01.001.